

Article

# Computational Treatments of Hybrid Dye Materials of Azobenzene and Chiral Schiff Base Metal Complexes

Takashiro Akitsu \*, Atsuo Yamazaki, Kana Kobayashi, Tomoyuki Haraguchi and Kazunaka Endo

Department of Chemistry, Faculty of Science, Tokyo University of Science, Tokyo 162-8601, Japan; guitarist-otohuke@hotmail.co.jp (A.Y.); akitsulab@gmail.com (K.K.); haraguchi@rs.tus.ac.jp (T.H.); endo\_kz@nifty.com (K.E.)

\* Correspondence: akitsu@rs.kagu.tus.ac.jp; Tel.: +81-3-5228-8271

Received: 8 March 2018; Accepted: 27 March 2018; Published: 28 March 2018



**Abstract:** Molecular orientation of dyes must be one of the important factors for designing dye-sensitized solar cells (DSSC). As model systems, we have prepared new hybrid materials composed of azobenzene (AZ) and chiral Schiff base Cu(II) complexes (**pn(S)Cu** and **pn(R)Cu**) in polymethyl methacrylate (PMMA) cast films. In addition to experimental results, in order to understand their behavior due to anisotropic alignment of them by linearly polarized UV light irradiation, the so-called Weigert effect, we treated theoretically and discussed based on computational chemistry and mathematical treatments (MD simulation and Bayesian statistics).

**Keywords:** azobenzene; Schiff base complexes; polarized light; computation; MD; Bayesian statistics

## 1. Introduction

In recent years, dye-sensitized solar cells (DSSCs) are important and promising renewable energy devices applying organic dyes. There are some current requirements of this technology with some recent outcomes in this field, such as (i) replacement of organic electrolytes [1] with aqueous ones [2]; (ii) use of bio-sourced materials [3,4]; and (iii) increase of stability through polymer electrolytes [5,6].

For about a decade, we have systematically investigated photofunctional organic/inorganic hybrid materials containing photochromic organic dyes, such as azobenzene (AZ) [7–11], disperse red 1 [11], spiropyran [12,13], and inorganic metal complexes, such as (chiral) Schiff base [14–18] (especially related to salen-type [19–22]) or other magnetic complexes [23–27]. To form hybrid systems in the solid state, in addition, polymer matrix, e.g., polymethyl methacrylate (PMMA) or polyvinyl alcohol (PVA) [23,28], were also employed. The hybrid systems could be enriched with photo-switching functions by photochromic organic compounds that were exhibiting various structural or electronic properties. Such materials are also possible to examine optical anisotropy with large degree of freedom due to the Weigert effect after linearly polarized UV light irradiation, similar to azo-containing polymers [29] or liquid crystals [30]. Thus, two kinds of light-irradiation methods (Weigert effect is only polarized UV light, while photoisomerization is alternate UV and visible light) are expected for these materials. In recent years, separated system of AZ and complexes as well as complexes having ligands of azobenzene-moiety were prepared. Among them, the types of Schiff base complexes, their central metal ions, stereochemical conformation deriving from ligands, or chirality (achiral meso-form, racemic ones, or optically active enantiomers), and intermolecular interactions between the solutes may be the dominating factors for controlling photo-induced molecular orientations.

By the way, to improve the photovoltaic performance of DSSC based on dyes, dye aggregation [31], in other words, mutual alignment [32] or orientation [33] of dye molecules, may be an essential factor to

design good devices beyond molecular level (adsorption on surface [34]) material design. Hence, even if employing the identical dyes, the performance may depend on molecular orientation of dyes, as well as their optically effective intermolecular interaction [35].

From this viewpoint of oriented dyes and chiral solutes [36], herein we prepared new organic/inorganic hybrid systems containing azobenzene (AZ) and sterically small chiral Schiff base Cu(II) complexes (**pn(S)Cu** and **pn(R)Cu**) in PMMA cast films (Figure 1). Besides, linearly polarized light induced molecular orientation like a previous study [19,22,31–33], their mathematical treatments in Bayesian statistics [34,35], and molecular modeling assuming in PMMA matrix by means of molecular dynamics (MD) simulation [37] will be mentioned.

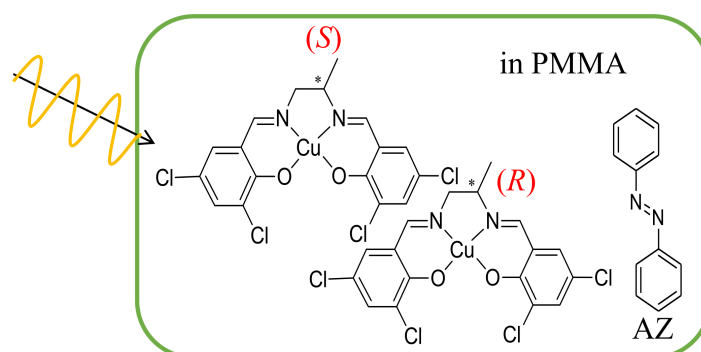


**Figure 1.** Schematic representation of organic/inorganic hybrid materials **pn(S)Cu** (or **pn(R)Cu**)+AZ+PMMA showing linearly polarized UV light irradiation for inducing anisotropic molecular orientation.

## 2. Results

### 2.1. Preparations of Chiral Cu(II) Complexes and Photofunctional Hybrid Materials

As for solely metal complexes, Figure 2 depicts circular dichroism (CD) and UV-vis spectra of **pn(R)Cu** and **pn(S)Cu** to confirm that they are enantiomers because of symmetric CD curves. With the aid of DFT calculations of the related complexes [20–22], the d–d, CT, and  $\pi$ – $\pi^*$  bands due to electric dipole transitions at about 550 nm, 400 nm, and 260 nm in UV-vis spectra (and also the corresponding CD spectra with slight deviation due to magnetic dipole transitions) could be assigned reasonably. Figure 3 exhibits the magnetic properties of **pn(S)Cu** [22], which indicates that it is merely a mononuclear Cu(II) complex of  $3d^9$  configuration with  $S = 1/2$  typically.

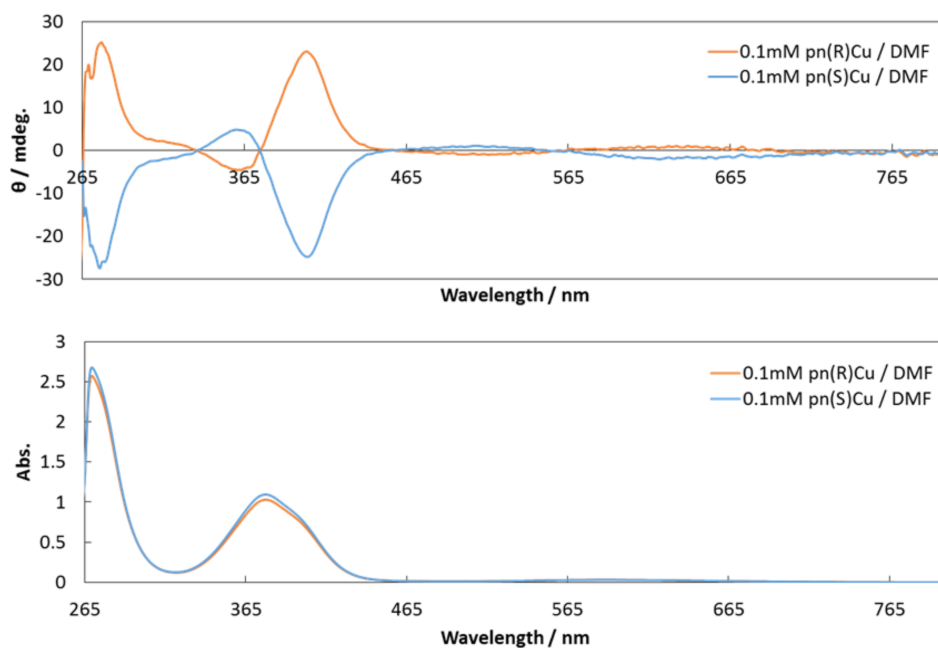


**Figure 2.** Circular dichroism (CD) (**above**) and UV-vis (**below**) spectra for **pn(R)Cu** and **pn(S)Cu** in 0.1 mM DMF solutions.

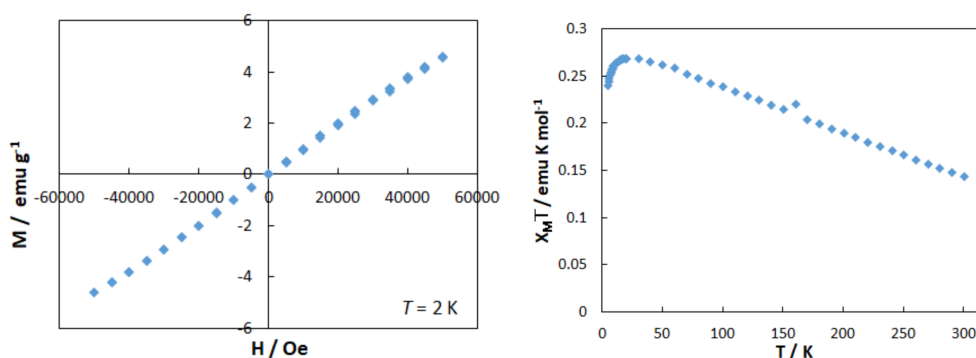


**Figure 3.** The  $M$  (magnetization) vs  $H$  (magnetic field) (**left**) and  $\chi_M T$  vs  $T$  (temperature) (**right**) curves for **pn(S)Cu**.

Figure 4 shows CD spectra for hybrid materials (**pn(R)Cu+AZ+PMMA** and **pn(S)Cu+AZ+PMMA** enantiomers and racemic **pn(R)Cu+pn(S)Cu+AZ+PMMA**, where **pn(R)Cu:pn(S)Cu = 1:1**). Because they are in the solid state, the artifact peak of LD and CD should interfere the observation of pure CD peaks [36]. However, qualitatively, opposite enantiomers and racemic materials indicated reasonable peaks, respectively. Additionally, Figure 5 depicts change of magnetic property of **pn(S)Cu+AZ+PMMA** before and after (natural, not polarized) UV light irradiation for 15 min.

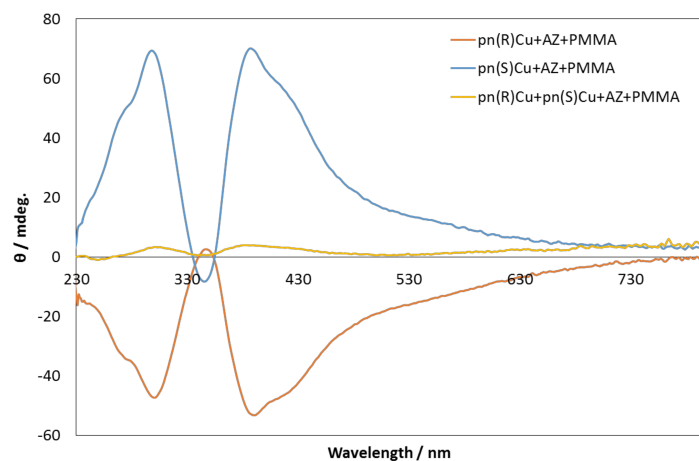


**Figure 4.** CD spectra of hybrid film materials of **pn(R)Cu+AZ+PMMA**, **pn(S)Cu+AZ+PMMA**, and racemic **pn(R)Cu+pn(S)Cu+AZ+PMMA**.

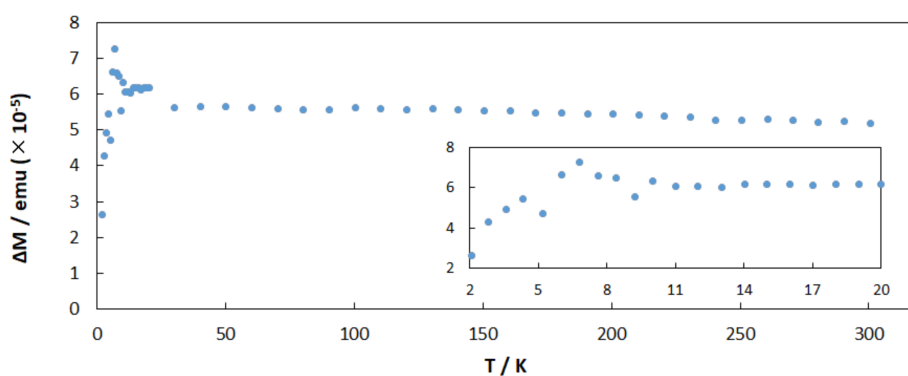


**Figure 5.** Change of magnetic property of **pn(S)Cu+AZ+PMMA**.  $\Delta M = M$  (after UV irradiation for 15 min) –  $M$  (before irradiation (0 min)).

Moreover, the *cis-trans* photoisomerization of **AZ** results in molecular mobility or motion in the **PMMA** matrix. This results in the intermolecular interactions decreasing the order and the aggregation in restricted environment (free volume) of **PMMA** films, which will be discussed with MD molecular modeling in a later section. It is examined that photoisomerization of **AZ** from *trans*-form to *cis*-form also resulted in slight increasing of magnetization [24–26]. The  $\Delta M$  value increases smoothly to a maximum value at 6.8 K, and then decreases sharply and reaches a minimum value at 2.1 K. The behavior supported the appropriate formation of hybrid materials, in other words, suitable dispersion and intermolecular interaction among the solutes.

## 2.2. Polarized UV Light Induced Molecular Alignment

The previous studies showed experimentally and discussed with computational chemistry [18,20]. Linearly polarized UV light irradiation leads to enhanced anisotropic molecular orientation, not only **AZ** directly, but also the complexes through intermolecular interaction in the **PMMA** matrix. In order to compare the degree of enhancing molecular orientation for **AZ** dyes and metal complexes, we compared polarized electronic spectra (some bands of dyes and complexes are overlapped) and polarized IR spectra (most of peaks are separated) for the hybrid materials. Figures 6 and 7 depict polarized IR or UV-vis spectra for **pn(R)Cu+pn(S)Cu+AZ+PMMA** and angular dependence of spectral intensity during rotation of polarizers, respectively. The C=N band and d–d band were shown for polarized IR spectra [38] and UV-vis spectra [39], respectively. Because these bands belong to metal complexes, the indirect interaction to them, differing from direct Weigert effect to **AZ**, were reflected

surely. However, the corresponding circularly polarized UV light did not induce supramolecular alignment of metal complexes clearly [29,30].

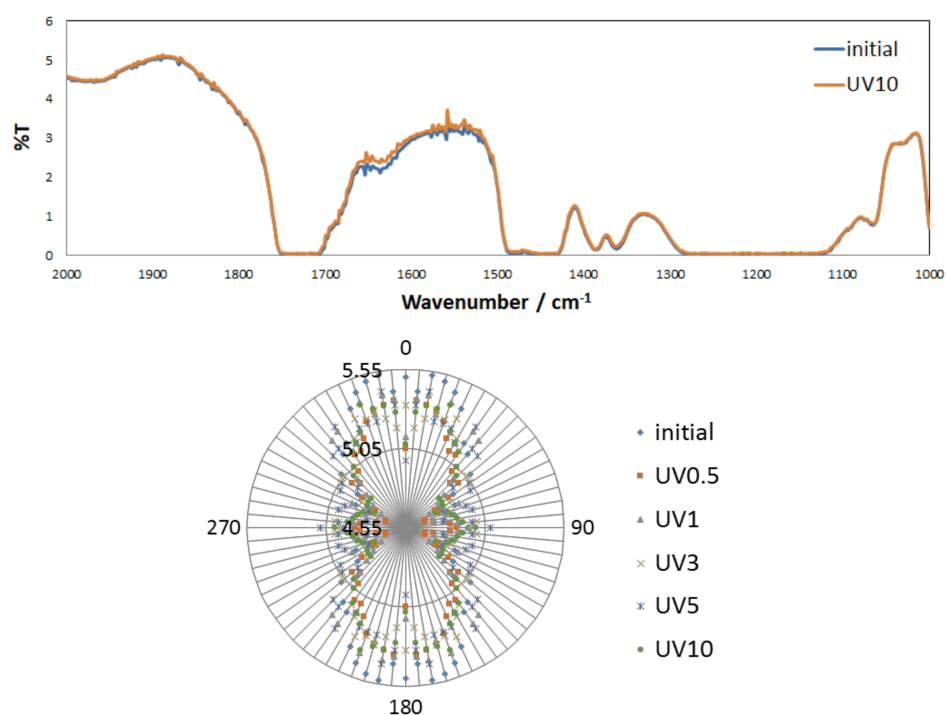


**Figure 6.** Change of polarized IR spectra (above) and (below) polarizer angular dependence of transmittance at C=N band ( $1633\text{ cm}^{-1}$ ) for  $\text{pn(R)Cu}+\text{pn(S)Cu}+\text{AZ}+\text{PMMA}$  up to 10 min polarized UV light irradiation.

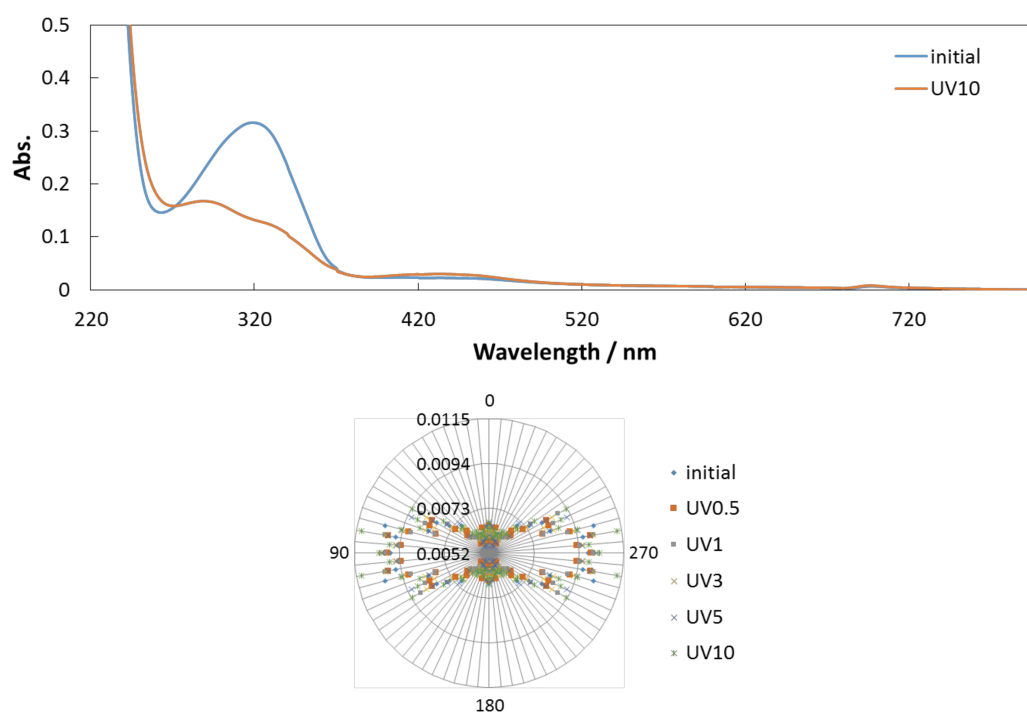


**Figure 7.** Change of polarized UV-vis spectra (above) and (below) polarizer angular dependence of absorbance at d-d band (587 nm) for  $\text{pn(R)Cu}+\text{pn(S)Cu}+\text{AZ}+\text{PMMA}$  up to 10 min polarized UV light irradiation.

For discussion of the Weigert effect, namely, the orientation of dyes in general and among many methods, we employed conventional polarized absorption spectra, and these two parameters ( $R$  and  $S$ ) for the degree of photo-induced optical anisotropy, in other words, spectral dichroism [11]:

$$R = \frac{A_0}{A_{90}};$$

$$S = \frac{A_0 - A_{90}}{A_0 + A_{90}},$$

where  $A_{90}$  and  $A_0$  denote the absorbance measured with the measuring polarizer perpendicular and parallel, respectively, to the electric vector of irradiation polarized light. For both polarized UV-vis and IR spectra, the ideal isotropic systems of  $S = 0$  and  $R = 1$  and both  $S$  and  $R$  parameters are changed as dichroism by molecular alignment increases.

It is well known that the *trans*-form is more stable than the *cis*-form. Within 3 min irradiation, optical anisotropy due to Weigert effect were saturated, in which most of AZ molecules may afford the *cis*-form. Detected with polarized UV-vis spectra, ( $R$  and  $S$ ) values at 3 min are (0.70 and  $-0.11$ ), (0.62 and  $-0.14$ ), and (0.63 and  $-0.14$ ) for **pn(R)Cu+AZ+PMMA**, **pn(S)Cu+AZ+PMMA**, and racemic **pn(R)Cu+pn(S)Cu+AZ+PMMA**, respectively. In contrast, detected with polarized IR spectra, ( $R$  and  $S$ ) values at 3 min are (1.10 and 0.032), (1.10 and 0.033) and (1.07 and 0.023) for **pn(R)Cu+AZ+PMMA**, **pn(S)Cu+AZ+PMMA**, and racemic **pn(R)Cu+pn(S)Cu+AZ+PMMA**, respectively.

### 3. Discussion

#### 3.1. Bayesian Statistics for Data Smoothing

As mentioned in a previous section, polarizer angular dependence of spectral intensity sometimes exhibits scattering significantly, which may lead to varying the  $R$  and  $S$  values widely. Hence, Bayesian statistics [37] is applied to confirm the accuracy of the data in this study, as follows [38,39].

##### 3.1.1. Bayesian Theorem

When making two phenomena  $E$  (experiment) with  $T$  (theory), the combination probability  $p(T, E)$  is expressed by a product of probability  $p(T)$  around 1 phenomenon [or,  $p(E)$ ] and other ex post facto probability  $p(E|T)$  [or,  $p(T|E)$ ].

$$p(T, E) = p(T)p(E|T) = p(E)p(T|E) \quad ()$$

$p(T)$ : The probability of previous phenomenon  $T$  that phenomenon  $E$  occurs (preliminary probability)

$p(E)$ : The probability of the previous phenomenon  $E$  that phenomenon  $T$  gets up (preliminary probability)

$p(E|T)$ : The probability of phenomenon  $E$  in later that phenomenon  $T$  got up (ex post facto probability or conditional probability)

$p(T|E)$ : The probability of phenomenon  $T$  at the back that phenomenon  $E$  has occurred (ex post facto probability or conditional probability)

When theory  $T$  is granted from the special system, one can understand ex post facto probability  $p$  in  $T(T|E)$  [the back probability that an experimental result was understood] to be proportional to a product of preliminary probability  $p(T)$  in  $T$  [the previous probability that an experimental result is understood] and ex post facto probability  $p(E|T)$  of an experimental result.

$$p(T|E) \propto p(T)p(E|T) \quad ()$$

##### 3.1.2. Application of Bayesian Theorem

- (1) A precondition: Inference of an anisotropy parameter of the phenomenon that forms by a fixation probability.

1. A phenomenon generates time  $t$  in fixation probability  $R \Delta t$  between minute time  $\Delta t$  which divided the  $m$  time.
  2. The phenomenon of which  $n$  is independent is observed in time  $t_i$  ( $i = 1, \dots, n$ ).
- (2) Bayes inference
1. Reverse ex post facto probability after the first phenomenon occurrence.
  2. The probability that a change in anisotropy occurs to a  $m$  time trial and it doesn't occur just before it.
  3.  $\Delta t$  gets a limit of 0,  $m$  is infinite,  $p, p$  considers that 0 ( $RR$ ) is a scale factor.
  4. When a phenomenon of a  $n$  time trial was observed in time  $t_n$ .
  5. A mean of observed time interval is  $\langle t \rangle$ , and the special system is integrated.

Further, a histogram/an accumulation distribution map for the experimental values was made. The probability density distribution function was calculated Bayesian theorem and this and the histogram made from experimental value/an accumulation distribution map was compared. In case of  $n = 4$ , a thing with the distribution near mutual knew the function concerned from in case of the compound material ( $\text{pn}(\mathbf{R})\text{Cu}+\text{AZ}+\text{PMMA}$ ) and the frequency of the measurement (0.74). In the case of  $n = 3$ , a thing with the distribution near mutual knew the function concerned from in case of the compound material ( $\text{pn}(\mathbf{R})\text{Cu}+\text{pn}(\mathbf{S})\text{Cu}+\text{AZ}+\text{PMMA}$ ) and the frequency of the measurement (0.65) (Figure 8 and Table 1). The thing to which nearby assessed value could be expressed is suggested by the parameter distributed, which becomes the dimension of the anisotropy parameter from the above.

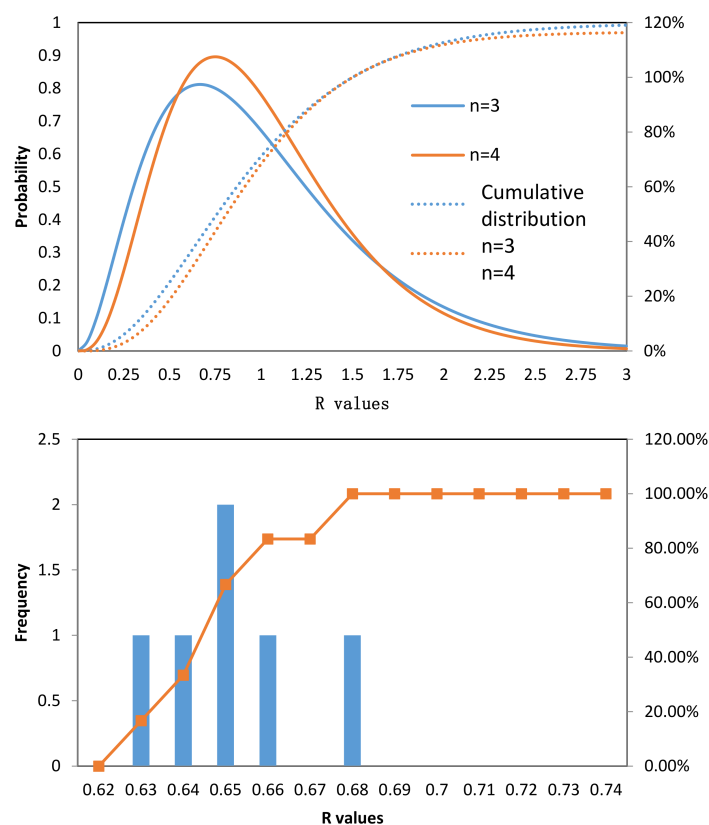


Figure 8. Correlation as probability (above) and frequency (below) for  $\text{pn}(\mathbf{R})\text{Cu}+\text{pn}(\mathbf{S})\text{Cu}+\text{AZ}+\text{PMMA}$ .

**Table 1.** Statistics data for **pn(S)Cu+AZ+PMMA** and **pn(R)Cu+pn(S)Cu+AZ+PMMA**.

	<b>pn(S)Cu+AZ+PMMA</b>	<b>pn(R)Cu+pn(S)Cu+AZ+PMMA</b>
Number of data	6	6
Average	0.71616	0.646637
Standard deviation	0.018778	0.01482
Median value	0.718471	0.6454
Frequency	0.74	0.65

### 3.2. MD Modeling of Hybrid Materials

Intermolecular interaction between the solute molecules strongly influenced the environment in a surrounding polymer matrix [40,41] In particular, it is important that intermolecular interactions are decreasing the order and the aggregation in restricted environment (free volume) of polymer films [42]. An orientation order and organization of the systems were examined by polarized spectroscopy, a statistical method (mentioned in a previous section), and molecular dynamics (MD) method [43], as following steps (Figure 9).

1. Systems 1, 2, 3 were modeled and calculated by a molecular dynamics method. After it is also judged as the one from temperature control (298 K) from the convergence situation of the energy. It was confirmed that a modeling of the system is proper.
2. Optically anisotropic of systems 1, 2, 3 were analyzed.

#### (1) Analysis result of system 1 (**AZ+PMMA**)

The molecule **AZ** was aligned under applied electric field. Optically anisotropy of 1 is larger than that of 2 and 3.

#### (2) Analysis result of system 2 (**pnCu(S)+PMMA**)

Molecular orientation in **pnCu(S)** underwent influence of applied electric field small, but it is begun from  $V = 10$ . A change wasn't indicated.

#### (3) Analysis result of system 3 (**pnCu(S)+AZ+PMMA**)

Optically anisotropic decreased and didn't change from  $V = 10$  as the whole system. **AZ** decreased as the details of the change in optically anisotropy, **pnCu(S)** is system 2. The Weigert effect of **AZ** could be assumed to occur within this timescale [42]. The effect of reorientation is for the one of the **pnCu(S)** molecules, which was not the driving force of a change of orientation.

According to the electric field that is applied ( $x$ -direction), the change in the size of the transition electric dipole moment of each system was analyzed (as a whole breakdown of the System 3, **AZ**, and **pnCu(S)** shown). In addition, the transition electric dipole moment of each system is the vector sum of the transition electric dipole moment of the individual molecules. The size of the transition electric dipole moment is standardized as a reference to the value at the time of the electric field 0. Dichroism is caused by an alignment of the dipole moments of the azo-compounds perpendicular to the polarization direction of irradiation polarized light [44,45]. Assuming molecular dipole moment of **AZ** or the related complexes based on calculations [46,47] as not photo-excited state [48], but merely ground state, expected total dipole moment were also confirmed to be aligned in the same direction in a qualitative manner as time advances in MD simulations (not shown).

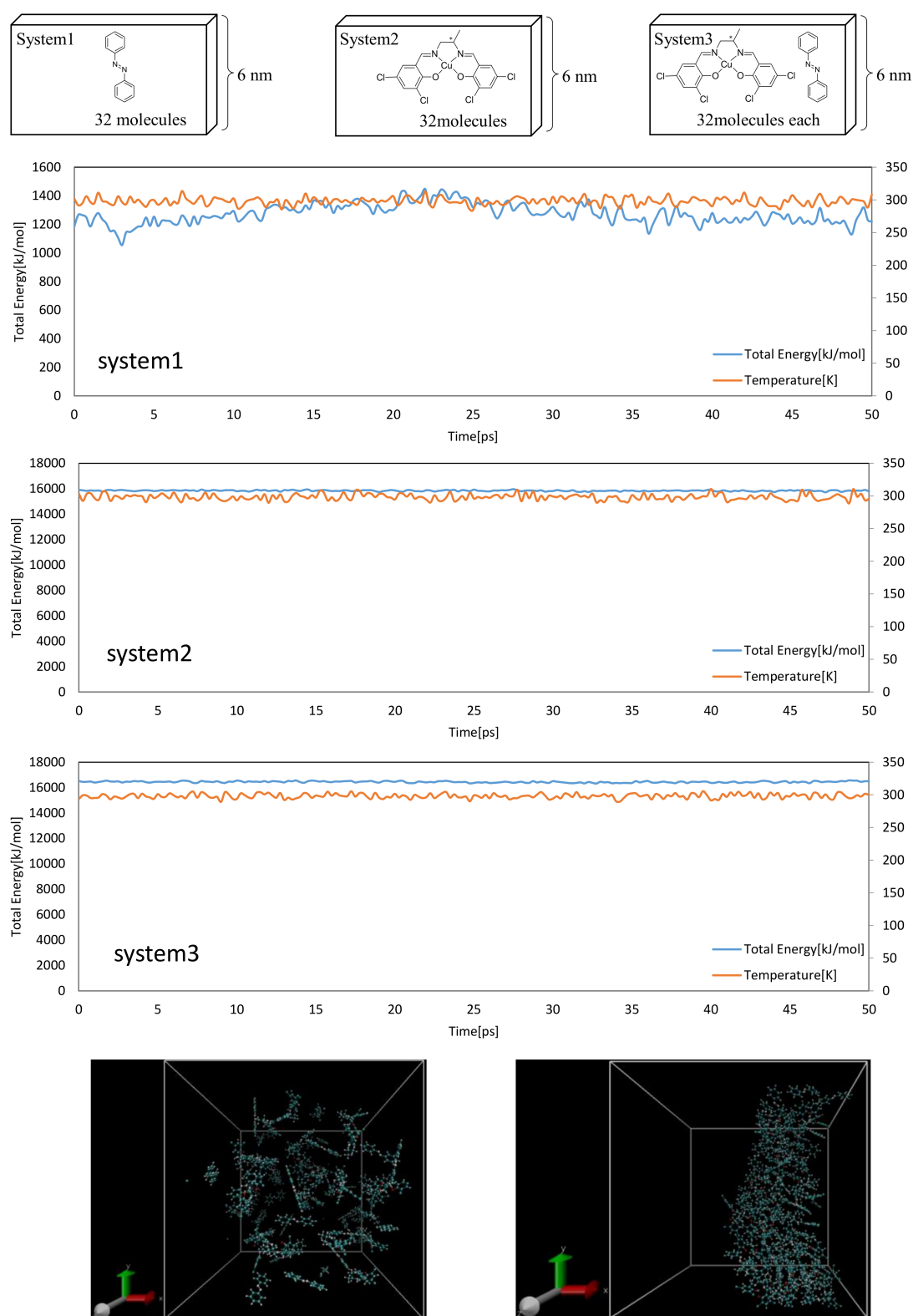


**Figure 9.** (Above) Molecules of systems 1–3; (Middle) Energy changes of systems 1–3; (Below) Visualized molecular modeling results of **pnCu(S)+AZ+PMMA** at 0 ps (left) and 50 ps (right).

#### 4. Materials and Methods

To a solution of 3,5-dichlorosalicylaldehyde (0.1910 g, 1.00 mmol) dissolved in methanol (50 mL), (S) or (R)-2-aminopropane (0.1272 g, 1.00 mmol) were added dropwise and stirred at 313 K for 2 h to give an orange solution of ligand. Copper acetate (II) acetate tetrahydrate (0.1244 g, 0.500 mmol) was added to the resulting solution to give an orange solution of the complex. After stirring for 2 h, this crude orange compound was filtered to give green microcrystals. **pn(S)Cu**: Yield: 38.4%. Anal. Found. C; 42.31, H; 2.49, N; 5.51, Calcd. C; 42.39, H; 2.51, N; 5.82 for  $C_{17}H_{12}Cl_4CuN_2O_2$ . IR (KBr):  $1633\text{ cm}^{-1}$  (C=N). Diffuse reflectance electronic spectra: 370 nm ( $\pi-\pi^*$ ), 562 nm (d-d). **pn(R)Cu**: Yield: 36.2%. Anal. Found. C; 42.42, H; 2.44, N; 5.50, Calcd. C; 42.39, H; 2.51, N; 5.82 for  $C_{17}H_{12}Cl_4CuN_2O_2$ . IR (KBr):  $1633\text{ cm}^{-1}$  (C=N). Diffuse reflectance electronic spectra: 369 nm ( $\pi-\pi^*$ ), 559 nm (d-d).

Elemental analyses were carried out with a Perkin-Elmer 2400II CHNS/O analyzer (Perkin-Elmer, Waltham, MA, USA) at Tokyo University of Science. Infrared (IR) spectra were recorded on a JASCO FT-IR 4200 plus spectrophotometer (JASCO, Tokyo, Japan), equipped with a polarizer in the range of  $4000-400\text{ cm}^{-1}$  at 298 K. Absorption electronic spectra were measured on a JASCO V-570 spectrophotometer equipped with a polarizer in the range of 900–200 nm at 298 K. Circular dichroism (CD) spectra were measured on a JASCO J-725 spectropolarimeter in the range of 800–200 nm at 298 K. Magnetic properties were investigated with a Quantum Design MPMS-XL superconducting quantum interference device magnetometer (SQUID, Quantum Design, San Diego, CA, USA) at an applied field 5000 G in the temperature range 2–300 K. The diamagnetic correction was carried out by using the Pascal constants. Photo-illumination was carried out using a lamp ( $1.0\text{ mW/cm}^2$ ) with optical filters (UV  $\lambda = 200-400\text{ nm}$ ) and a polarizer.

Modeling of target molecules was carried out using above-mentioned quantum chemical methods. After confirming the convergence of energy of modeling structure by gradient descent method, MD simulation was performed using GROMACS (Ver. 5.0.4, University of Groningen, Royal Institute of Technology, Uppsala University, Groningen, The Netherlands) [49].

#### 5. Conclusions

In summary, as a basic model system of orientation effects containing multiple (colourful) DSSC dyes [50,51], chiral Schiff base Cu(II) complexes and **AZ** were also observed their increase in optical anisotropy as organic/inorganic composites in PMMA films. We have tried the observation of optical anisotropy by polarized UV light irradiation and the new theoretical approaches for appropriate treatments. Intermolecular interaction and mechanism concerning molecular orientation of solutes in **PMMA** were improved with the Bayesian theorem and simulated using MD modelling, respectively. Indeed, such intermolecular interaction between dye molecules should be important in co-sensitization [52] or other material design application (for example, donor-acceptor dye systems in polymers [53,54]) for DSSC.

**Acknowledgments:** The computations were performed at the Research Center for Computational Science, Okazaki, Japan.

**Author Contributions:** Takashiro Akitsu designed the study and wrote the paper; Tomoyuki Haraguchi wrote the paper; Kana Kobayashi performed experiments; Atsuo Yamazaki and Kazunaka Endo designed and performed theoretical and computational works.

**Conflicts of Interest:** The authors declare no conflict of interest.

## Abbreviations

The following abbreviations are used in this manuscript:

AZ	azobenzene
CD	circular dichroism
IR	infrared
PMMA	polymethyl methacrylate
MD	molecular dynamics
UV	ultraviolet
Vis	visible

## References

1. Mustafa, M.N.; Shafie, S.; Zainal, Z.; Sulaiman, Y. Poly(3,4-ethylenedioxythiophene) doped with various carbon-based materials as counter electrodes for dye sensitized solar cells. *Mater. Des.* **2017**, *136*, 249–257. [[CrossRef](#)]
2. Najafi-Ghalelou, A.; Nojavan, S.; Zare, K. Finely tuning electrolytes and photoanodes in aqueous solar cells by experimental design. *Sol. Energy* **2018**, *163*, 251–255.
3. Salvador, G.P.; Pugliese, D.; Bella, F.; Chiappone, A.; Sacco, A.; Bianco, S.; Quaglio, M. New insights in long-term photovoltaic performance characterization of cellulose-based gel electrolytes for stable dye-sensitized solar cells. *Electrochim. Acta* **2014**, *146*, 44–51. [[CrossRef](#)]
4. Bella, F.; Chiappone, A.; Nair, J.R.; Meligrana, G.; Gerbaldi, C. Effect of Different Green Cellulosic Matrices on the Performance of Polymeric Dye-Sensitized Solar Cells. *Chem. Eng. Trans.* **2014**, *41*, 211–216.
5. Imperiyka, M.; Ahmad, A.; Hanifah, S.A.; Bella, F. A UV-prepared linear polymer electrolyte membrane for dye-sensitized solar cells. *Phys. B Condens. Matter* **2014**, *450*, 151–154. [[CrossRef](#)]
6. Bella, F.; Galliano, S.; Falco, M.; Viscardi, G.; Barolo, C.; Grätzel, M.; Gerbaldi, C. Approaching truly sustainable solar cells by the use of water and cellulose derivatives. *Green Chem.* **2017**, *19*, 1043–1051. [[CrossRef](#)]
7. Akitsu, T.; Einaga, Y. Syntheses, crystal structures, and electronic properties of a series of copper(II) complexes with 3,5-halogen-substituted Schiff base ligands and their solutions. *Polyhedron* **2005**, *24*, 2933–2943. [[CrossRef](#)]
8. Akitsu, T.; Einaga, Y. Synthesis, crystal structures, and electronic properties of Schiff base nickel(II) complexes: Towards solvatochromism induced by photochromic solute. *Polyhedron* **2005**, *24*, 1869–1877. [[CrossRef](#)]
9. Akitsu, T. Photofunctional supramolecular solution systems of chiral Schiff base nickel(II), copper(II), and zinc(II) complexes and photochromic azobenzenes. *Polyhedron* **2007**, *26*, 2527–2535. [[CrossRef](#)]
10. Akitsu, T.; Itoh, T. Polarized spectroscopy of hybrid materials of chiral Schiff base cobalt(II), nickel(II), copper(II), and zinc(II) complexes and photochromic azobenzenes in PMMA films. *Polyhedron* **2010**, *29*, 477–487. [[CrossRef](#)]
11. Akitsu, T.; Ishioka, C.; Itoh, T. Polarized Spectroscopy of Hybrid Materials of Mn<sub>12</sub> Single-Molecule Magnet and Azobenzene or Disperse Red 1 in PMMA Films. *Cent. Eur. J. Chem.* **2009**, *7*, 690. [[CrossRef](#)]
12. Akitsu, T.; Tanaka, R. Polarized Electronic and IR Spectra of Hybrid Materials of Chiral Mn(II) Complexes and Different Types of Photochromic Dyes Showing Photoisomerization or Weigert Effect. *Curr. Phys. Chem.* **2011**, *1*, 82–89. [[CrossRef](#)]
13. Miura, T.; Onodera, T.; Endo, S.; Yamazaki, A.; Akitsu, T. Some hybrid systems of chiral Schiff base Zn(II) complexes and photochromic spiropyranes for environmental ion sensing. *Am. J. Anal. Chem.* **2014**, *5*, 751–765. [[CrossRef](#)]
14. Aritake, Y.; Takanashi, T.; Yamazaki, A.; Akitsu, T. Polarized spectroscopy and hybrid materials of chiral Schiff base Ni(II), Cu(II), Zn(II) complexes with included or separated azo-groups. *Polyhedron* **2011**, *30*, 886–894. [[CrossRef](#)]
15. Aritake, Y.; Akitsu, T. The role of chiral dopants in organic/inorganic hybrid materials containing chiral Schiff base Ni(II), Cu(II), and Zn(II) complexes. *Polyhedron* **2012**, *31*, 278–284. [[CrossRef](#)]
16. Ito, M.; Akitsu, T. Polarized UV light induced molecular arrangement depending on flexibility of chiral Schiff base Ni(II), Cu(II), and Zn(II) complexes by azobenzene in PMMA matrix. *Contemp. Eng. Sci.* **2014**, *7*, 869–877. [[CrossRef](#)]

17. Hariu, N.; Ito, M.; Akitsu, T. Linearly, Circularly, or Non-polarized Light Induced Supramolecular Arrangement of Diastereomer Schiff Base Ni(II), Cu(II), and Zn(II) Complexes by Azobenzene in PMMA Matrix. *Contemp. Eng. Sci.* **2015**, *8*, 57–70. [[CrossRef](#)]
18. Ito, M.; Akitsu, T.; Palafox, M.A. Theoretical interpretation of polarized light-induced supramolecular orientation on the basis of normal mode analysis of azobenzene as hybrid materials in PMMA with chiral Schiff base Ni(II), Cu(II), and Zn(II) complexes. *J. Appl. Solut. Chem. Model.* **2016**, *5*, 30–47.
19. Akitsu, T.; Tanaka, R.; Yamazaki, A. Separate observation with polarized electronic and IR spectra of hybrid materials of chiral Mn(II) complexes and azobenzene. *J. Mater. Sci. Eng. A* **2011**, *1*, 518–525.
20. Yamazaki, A.; Akitsu, T. Polarized spectroscopy and polarized UV light-induced molecular orientation of chiral diphenyl Schiff base Ni(II) and Cu(II) complexes and azobenzene in a PMMA film. *RSC Adv.* **2012**, *2*, 2975–2980. [[CrossRef](#)]
21. Yamazaki, A.; Hiratsuka, T.; Akitsu, T. Computational details of calculated UV-VIS and CD spectra of a salen type of chiral Schiff base Ni(II) complex. *Asian Chem. Lett.* **2012**, *16*, 1–8.
22. Yamazaki, A.; Hiratsuka, T.; Akitsu, T. Computational UV-VIS and CD spectra of a chiral Schiff base mononuclear Cu(II) complex (salpn). *Asian Chem. Lett.* **2012**, *16*, 19–32.
23. Akitsu, T.; Einaga, Y. Novel photo-induced aggregation behavior of a supramolecular system containing iron(III) magnetic ionic liquid and azobenzene. *Inorg. Chem. Commun.* **2006**, *9*, 1108–1110. [[CrossRef](#)]
24. Aktisu, T.; Nishijo, J. The first observation of photoinduced tuning of AC magnetization for organic/inorganic hybrid materials composed of Mn<sub>12</sub>-acetate and azobenzene. *J. Magn. Magn. Mater.* **2007**, *315*, 95–100. [[CrossRef](#)]
25. Aktisu, T.; Nishijo, J. The first detection of photomodulation by both DC and in-phase AC susceptibility for organic/inorganic hybrid materials containing cyano-bridged Gd–Cr complex and azobenzene. *J. Magn. Magn. Mater.* **2008**, *320*, 1586–1590. [[CrossRef](#)]
26. Aktisu, T. The tuning of quantum magnetization for organic/inorganic hybrid materials composed of Mn<sub>12</sub>-acetate and azobenzene casted into PMMA films on PVA films. *J. Magn. Magn. Mater.* **2009**, *321*, 207–212. [[CrossRef](#)]
27. Akitsu, T.; Tanaka, R. Polarized Electronic and IR Spectroscopy of Hybrid Materials of Chiral Cu(II) and Mn<sub>12</sub> Complexes and Some Photochromic Compounds in PMMA Films. *Asian Chem. Lett.* **2010**, *14*, 235–254.
28. Takase, M.; Akitsu, T. Linearly polarized light-induced anisotropic orientation of binuclear Ni(II), Cu(II), and Zn(II) Schiff base complexes including or without methyl orange in PVA. In *Polymer Science Book Series—Volume # 1: “Polymer Science: Research Advances, Practical Applications and Educational Aspects”*; Formatex Research Centre: Badajoz, Spain, 2016; pp. 301–308.
29. Natansohn, A.; Rochon, P. Photoinduced Motions in Azo-Containing Polymers. *Chem. Rev.* **2002**, *102*, 4139–4175. [[CrossRef](#)] [[PubMed](#)]
30. Ichimura, K. Photoalignment of Liquid-Crystal Systems. *Chem. Rev.* **2000**, *100*, 1847–1874. [[CrossRef](#)] [[PubMed](#)]
31. Zhang, L.; Cole, J.M. Dye aggregation in dye-sensitized solar cells. *J. Mater. Chem. A* **2017**, *5*, 19541–19559. [[CrossRef](#)]
32. Ooyama, Y.; Shimada, Y.; Inoue, S.; Nagano, T.; Fujikawa, Y.; Komaguchi, K.; Imae, I.; Harima, Y. New molecular design of donor- $\pi$ -acceptor dyes for dye-sensitized solar cells: Control of molecular orientation and arrangement on TiO<sub>2</sub> surface. *New J. Chem.* **2011**, *35*, 111–118. [[CrossRef](#)]
33. McCree-Grey, J.; Cole, J.M.; Evans, P.J. Preferred Molecular Orientation of Coumarin 343 on TiO<sub>2</sub> Surfaces: Application to Dye-Sensitized Solar Cells. *ACS Appl. Mater. Interfaces* **2015**, *7*, 16404–16409. [[CrossRef](#)] [[PubMed](#)]
34. Zhu, H.-C.; Zhang, J.; Wang, Y.-L. Adsorption orientation effects of porphyrin dyes on the performance of DSSC: Comparison of benzoic acid and tropolone anchoring groups binding onto the TiO<sub>2</sub> anatase (101) surface. *Appl. Surf. Sci.* **2018**, *433*, 1137–1147. [[CrossRef](#)]
35. Xu, X.; Cui, J.; Han, J.; Zhan, J.; Zhang, Y.; Luan, L.; Alemu, G.; Wang, Z.; Shen, Y.; Xiong, D.; et al. Near Field Enhanced Photocurrent Generation in p-type Dye-Sensitized Solar Cells. *Sci. Rep.* **2014**, *4*, 3961. [[CrossRef](#)] [[PubMed](#)]
36. Schellman, J.; Jensen, H.P. Optical spectroscopy of oriented molecules. *Chem. Rev.* **1987**, *87*, 1359–1399. [[CrossRef](#)]
37. Menten, T. Use of Bayesian Approach in Chemistry. *Hacet. J. Biol. Chem.* **2011**, *39*, 19–22.
38. Yamazaki, A.; Akitsu, T. Recent Treatment of Data in Chemical Analysis. *Trends Green Chem.* **2017**, *3*. [[CrossRef](#)]
39. Yamazaki, A.; Akitsu, T. Bayesian Statistics in Data Separation of Indicators for Neutralization Titration. *IJCST* **2017**, *104*. [[CrossRef](#)]

40. Sunaga, N.; Akitsu, T.; Konomi, T.; Katoh, M. The theoretical interpretation of the Linear/circularly polarized light-induced molecular orientation of the azo group-containing *trans*-Achiral Schiff base dinuclear complex composite material. *MATEC Web Conf.* **2017**, *130*, 07004. [[CrossRef](#)]
41. Takano, H.; Takase, M.; Sunaga, N.; Ito, M.; Akitsu, T. Viscosity and intermolecular interaction of organic/inorganic hybrid systems composed of chiral Schiff base Ni(II), Cu(II), Zn(II) complexes having long ligands, azobenzene and PMMA. *Inorganics* **2016**, *4*, 20. [[CrossRef](#)]
42. Van der Asdonk, P.; Kouwer, P.H.J. Liquid crystal templating as an approach to spatially and temporally organise soft matter. *Chem. Soc. Rev.* **2017**, *46*, 5935–5949. [[CrossRef](#)] [[PubMed](#)]
43. Berendsen, H.J.C. Biophysical Applications of Molecular Dynamics. *Compt. Phys. Commun.* **1987**, *44*, 233–242. [[CrossRef](#)]
44. Ivanova, B.; Kolev, T. *Linearly Polarized IR Spectroscopy Theory and Applications for Structural Analysis*; CRC Press: New York, NY, USA, 2012.
45. Norden, B.; Todger, A.; Dafforn, T. *Linear Dichroism and Circular Dichroism: A Textbook on Polarized-Light Spectroscopy*; RSC Publishing: London, UK, 2010.
46. Yamazaki, A.; Akitsu, T. Semiempirical molecular orbital calculations for 3d–4f complexes towards artificial metalloproteins. *Int. J. Pharma Sci. Sci. Res.* **2017**, *3*, 53–54.
47. Akitsu, T.; Yamazaki, A.; Hiroki, H. Drug Design Based on Unfitted or Repulsive Metal Complexes. *EC Pharmacol. Toxicol.* **2017**, *RCO.01*, 1–2.
48. Adamo, C.; Jacquemin, D. The calculations of excited-state properties with Time-Dependent Density Functional Theory. *Chem. Soc. Rev.* **2013**, *42*, 845–856. [[CrossRef](#)] [[PubMed](#)]
49. Pronk, S.; Páll, S.; Schulz, R.; Larsson, P.; Bjelkmar, P.; Apostolov, R.; Shirts, M.R.; Smith, J.C.; Kasson, P.M.; van der Spoel, D.; Hess, B.; Lindahl, E. GROMACS 4.5: A high-throughput and highly parallel open source molecular simulation toolkit. *Bioinformatics* **2013**, *29*, 845–854. [[CrossRef](#)] [[PubMed](#)]
50. Yamane, S.; Hiyoshi, Y.; Tanaka, S.; Ikenomoto, S.; Numata, T.; Takakura, K.; Haraguchi, T.; Palafox, M.A.; Hara, M.; Sugiyama, M. Substituent Effect of Chiraldiphenyl Salen Metal (M = Fe(II), Co(II), Ni(II), Cu(II), Zn(II)) Complexes for New Conceptual DSSC Dyes. *J. Chem. Chem. Eng.* **2018**, *11*, 135–151.
51. Yamaguchi, M.; Tsunoda, Y.; Tanaka, S.; Haraguchi, T.; Sugiyama, M.; Noor, S.; Akitsu, T. Molecular design through orbital and molecular design of new naphthyl-salen type transition metal complexes toward DSSC dyes. *J. Indian Chem. Soc.* **2017**, *94*, 761–772.
52. Yu, L.; Fan, K.; Duan, T.; Chen, X.; Li, R.; Peng, T. Efficient Panchromatic Light Harvesting with Co-Sensitization of Zinc Phthalocyanine and Bithiophene-Based Organic Dye for Dye-Sensitized Solar Cells. *ACS Sustain. Chem. Eng.* **2014**, *2*, 718–725. [[CrossRef](#)]
53. Zhang, T.; Guan, W.; Yan, L.; Ma, T.; Wang, J.; Su, Z. Theoretical studies on POM-based organic–inorganic hybrids containing double D–A1– $\pi$ –A2 chains for high-performance p-type, dye-sensitized solar cells (DSSCs). *Phys. Chem. Chem. Phys.* **2015**, *17*, 5459–5465. [[CrossRef](#)] [[PubMed](#)]
54. Jia, Y.; Gou, F.; Fang, R.; Jing, H.; Zhu, Z. SalenZn-bridged D- $\pi$ -A Dyes for Dye-Sensitized Solar Cells. *Chin. J. Chem.* **2014**, *31*, 513–520. [[CrossRef](#)]

